



HAL
open science

CD34+ mesenchymal cells are a major component of the intestinal stem cells niche at homeostasis and after injury.

Igor Stzepourginski, Giulia Nigro, Jean-Marie Jacob, Sophie Dulauroy, Philippe Sansonetti, Gérard Eberl, Lucie Peduto

► To cite this version:

Igor Stzepourginski, Giulia Nigro, Jean-Marie Jacob, Sophie Dulauroy, Philippe Sansonetti, et al.. CD34+ mesenchymal cells are a major component of the intestinal stem cells niche at homeostasis and after injury.. Proceedings of the National Academy of Sciences of the United States of America, 2017, 114 (4), pp.E506-E513. 10.1073/pnas.1620059114 . pasteur-01449402

HAL Id: pasteur-01449402

<https://pasteur.hal.science/pasteur-01449402>

Submitted on 7 Feb 2017

HAL is a multi-disciplinary open access archive for the deposit and dissemination of scientific research documents, whether they are published or not. The documents may come from teaching and research institutions in France or abroad, or from public or private research centers.

L'archive ouverte pluridisciplinaire **HAL**, est destinée au dépôt et à la diffusion de documents scientifiques de niveau recherche, publiés ou non, émanant des établissements d'enseignement et de recherche français ou étrangers, des laboratoires publics ou privés.



Distributed under a Creative Commons Attribution - NonCommercial - ShareAlike 4.0 International License

CD34⁺ mesenchymal cells are a major component of the intestinal stem cells niche at homeostasis and after injury

Igor Stjepourginski^{a,b,c}, Giulia Nigro^{d,e}, Jean-Marie Jacob^{a,c}, Sophie Dulauroy^{b,c}, Philippe J. Sansonetti^{d,e,f,1}, Gérard Eberl^{b,c}, and Lucie Peduto^{a,c,1}

^aUnité Stroma, Inflammation & Tissue Repair, Institut Pasteur, 75724 Paris, France; ^bUnité Microenvironnement & Immunity, Institut Pasteur, 75724 Paris, France; ^cINSERM U1224, 75724 Paris, France; ^dUnité de Pathogénie Microbienne Moléculaire, Institut Pasteur, 75724 Paris, France; ^eINSERM U1202, 75724 Paris, France; and ^fChaire de Microbiologie et Maladies Infectieuses, Collège de France, 75231 Paris, France

Contributed by Philippe J. Sansonetti, December 8, 2016 (sent for review October 6, 2016; reviewed by Andreas J. Bäumlér and Maria Rescigno)

The intestinal epithelium is continuously renewed by intestinal epithelial stem cells (I ESCs) positioned at the base of each crypt. Mesenchymal-derived factors are essential to maintain I ESCs; however, the cellular composition and development of such mesenchymal niche remains unclear. Here, we identify pericryptal CD34⁺ Gp38⁺ αSMA⁻ mesenchymal cells closely associated with Lgr5⁺ I ESCs. We demonstrate that CD34⁺ Gp38⁺ cells are the major intestinal producers of the niche factors Wnt2b, Gremlin1, and R-spondin1, and are sufficient to promote maintenance of Lgr5⁺ I ESCs in intestinal organoids, an effect mainly mediated by Gremlin1. CD34⁺ Gp38⁺ cells develop after birth in the intestinal submucosa and expand around the crypts during the third week of life in mice, independently of the microbiota. We further show that pericryptal CD34⁺ Gp38⁺ cells are rapidly activated by intestinal injury, up-regulating niche factors Gremlin1 and R-spondin1 as well as chemokines, proinflammatory cytokines, and growth factors with key roles in gut immunity and tissue repair, including IL-7, Ccl2, Ptg2, and Amphiregulin. Our results indicate that CD34⁺ Gp38⁺ mesenchymal cells are programmed to develop in the intestine after birth to constitute a specialized microenvironment that maintains I ESCs at homeostasis and contribute to intestinal inflammation and repair after injury.

intestinal stem cells | mesenchymal niche | inflammation | CD34

The adult intestinal epithelium is one of the most rapidly self-renewing tissues in mammals. Intestinal epithelial cells renewal is ensured by intestinal epithelial stem cells (I ESCs) located in the crypts and identified by expression of Lgr5 (1). I ESCs are responsible for the continuous production of rapidly dividing transit-amplifying (TA) cells and of Paneth cells while maintaining the size of their own population. Upon leaving the crypts, TA cells proliferate and migrate upwards, differentiating into enterocytes, goblet cells, Tuft cells, and enteroendocrine cells, before undergoing apoptosis at the villus tip and being shed into the intestinal lumen (2).

A complex gradient of factors maintains I ESC stemness and proliferation, and supports enterocyte differentiation along the crypt-villus axis. Notably, Wnt signals are required to maintain the I ESC niche (3, 4). In the crypts, Paneth cells express factors that promote stem cells growth, including the Wnt ligand Wnt3a, Notch ligands (Dll4, Dll1), and epidermal growth factor (EGF) (3, 5, 6). In addition, a number of factors produced by mesenchymal cells have an essential role in the maintenance of I ESCs such as Wnt2b, a canonical Wnt ligand that activates the Wnt/β-catenin pathway (7); the Lgr4/5 ligand R-spondin1 (Rspo1), a strong mitogen for Wnt-responsive intestinal crypts (8–10); and Gremlin1 (Grem1), a bone morphogenetic protein (BMP) antagonist (11, 12). As epithelial cells ascend the crypt, BMPs produced by alpha-smooth muscle actin positive (αSMA⁺) myofibroblasts restrain Wnt-induced epithelial proliferation while promoting their differentiation into secretory or absorptive epithelial cells

(13, 14). Whereas αSMA⁺ myofibroblasts are the main source for BMPs (15), the cellular composition of the I ESC niche remains unclear. Notably, ablation of Paneth cells does not affect the function of I ESCs and mice lacking Wnt activity in epithelial cells or myofibroblastic cells have normal intestinal homeostasis (16–18), indicating an essential role for nonepithelial and nonmyofibroblastic populations.

Here, we identify CD34⁺ Gp38⁺ mesenchymal cells as the major intestinal source for the niche factors Wnt2b, Grem1, and Rspo1. CD34⁺ Gp38⁺ cells are closely associated with Lgr5⁺ I ESCs in mouse colon and ileum, and are sufficient to induce expansion of Lgr5⁺ I ESCs while blocking epithelial differentiation in intestinal organoids, an effect mainly mediated by Grem1. CD34⁺ Gp38⁺ cells are topographically and functionally distinct from αSMA⁺ subepithelial myofibroblasts, they develop after birth in the submucosa, and expand around crypts during the third week after birth, in a process independent of the microbiota and recognition of microbe-associated molecular patterns (MAMPs). After dextran sodium sulfate (DSS)-induced colitis, CD34⁺ Gp38⁺ cells remain associated to crypts and strongly up-regulate niche factors Grem1 and Rspo1, as well as chemokines, cytokines, and growth factors with essential roles in gut inflammation and repair. Our results indicate that CD34⁺ Gp38⁺ mesenchymal cells develop after birth in the intestine to create a niche that maintains I ESCs at homeostasis and

Significance

Maintenance of stem cells in adult organs requires a specialized microenvironment called the niche, which provides structural cues and paracrine signals to ensure stemness. In the intestine, increasing evidence points toward a major role for the mesenchyme close to crypts to perform this function; however, such putative mesenchymal niche remains poorly characterized. Here, we identify nonmyofibroblastic CD34⁺ Gp38⁺ mesenchymal cells as a major component of the intestinal epithelial stem cells (I ESCs) niche. We show that CD34⁺ Gp38⁺ mesenchymal cells develop after birth and contribute to the maintenance of I ESCs at homeostasis and organization of intestinal inflammation after injury.

Author contributions: I.S., G.N., P.J.S., G.E., and L.P. designed research; I.S., G.N., J.-M.J., and S.D. performed research; I.S., G.N., J.-M.J., S.D., P.J.S., G.E., and L.P. analyzed data; and I.S., G.E., and L.P. wrote the paper.

Reviewers: A.J.B., University of California-Davis; and M.R., European Institute of Oncology.

The authors declare no conflict of interest.

Freely available online through the PNAS open access option.

¹To whom correspondence may be addressed. Email: lucie.peduto@pasteur.fr or philippe.sansonetti@pasteur.fr.

This article contains supporting information online at www.pnas.org/lookup/suppl/doi:10.1073/pnas.1620059114/-DCSupplemental.

contribute to host defense and tissue repair upon intestinal damage.

Results

Coexpression of gp38 and CD34 Identifies Pericryptal α SMA⁻ Mesenchymal Cells. We showed that expression of gp38 (podoplanin) identifies a major fraction of mesenchymal cells of the intestinal lamina propria (19, 20). Because lymphatic endothelial cells (LECs) also express gp38 (21), we used a combination of gp38 and CD31, a marker for endothelial cells, to identify gp38⁺ CD31⁻ mesenchymal cells. We observed that gp38⁺ mesenchymal cells (gp38⁺ stroma) accounted for up to 73% of total non-hematopoietic (CD45⁻) cells in the adult mouse colon (Fig. 1A, Left) and ileum (Fig. S14, Left). A subpopulation of gp38⁺ stromal cells coexpressed CD34 (Fig. 1A, Right and Fig. S14, Right), a marker also expressed by endothelial cells (22), mesenchymal stem cells (23) and human intestinal mesenchyme (24). Gp38⁺CD34⁺

double positive stromal cells were localized near the crypts in colon (orange-yellow staining in Fig. 1B, Left) and ileum (Fig. 1B, Right) (thereafter called CD34⁺ CSCs for crypt stromal cells), in close contact with Lgr5⁺ stem cells (Fig. 1C), and were α SMA^{-low} (arrows in Fig. 1D and E, Top; analysis of α SMA expression by intracellular FACS analysis is shown in Fig. S1B). In contrast, gp38⁺ CD34⁻ stromal cells were mainly found in the lamina propria of the upper villi and colon tops (Fig. 1B, green staining) and were mostly α SMA^{high} (arrowheads in Fig. 1D and E, Bottom and Fig. S1B), a defining characteristic of α SMA⁺ subepithelial myofibroblasts (15), and are thereafter called CD34⁻ MyoFs. Single positive CD34⁺gp38⁻ cells in the crypts and villi were blood endothelial cells (Fig. S1C).

Subepithelial α SMA⁺ myofibroblasts play a major role in promoting intestinal epithelial differentiation through secretion of BMPs (25, 26). Consistent with their pericryptal localization and low expression of α SMA, CD34⁺ CSCs isolated from the intestinal lamina propria expressed significantly lower levels of

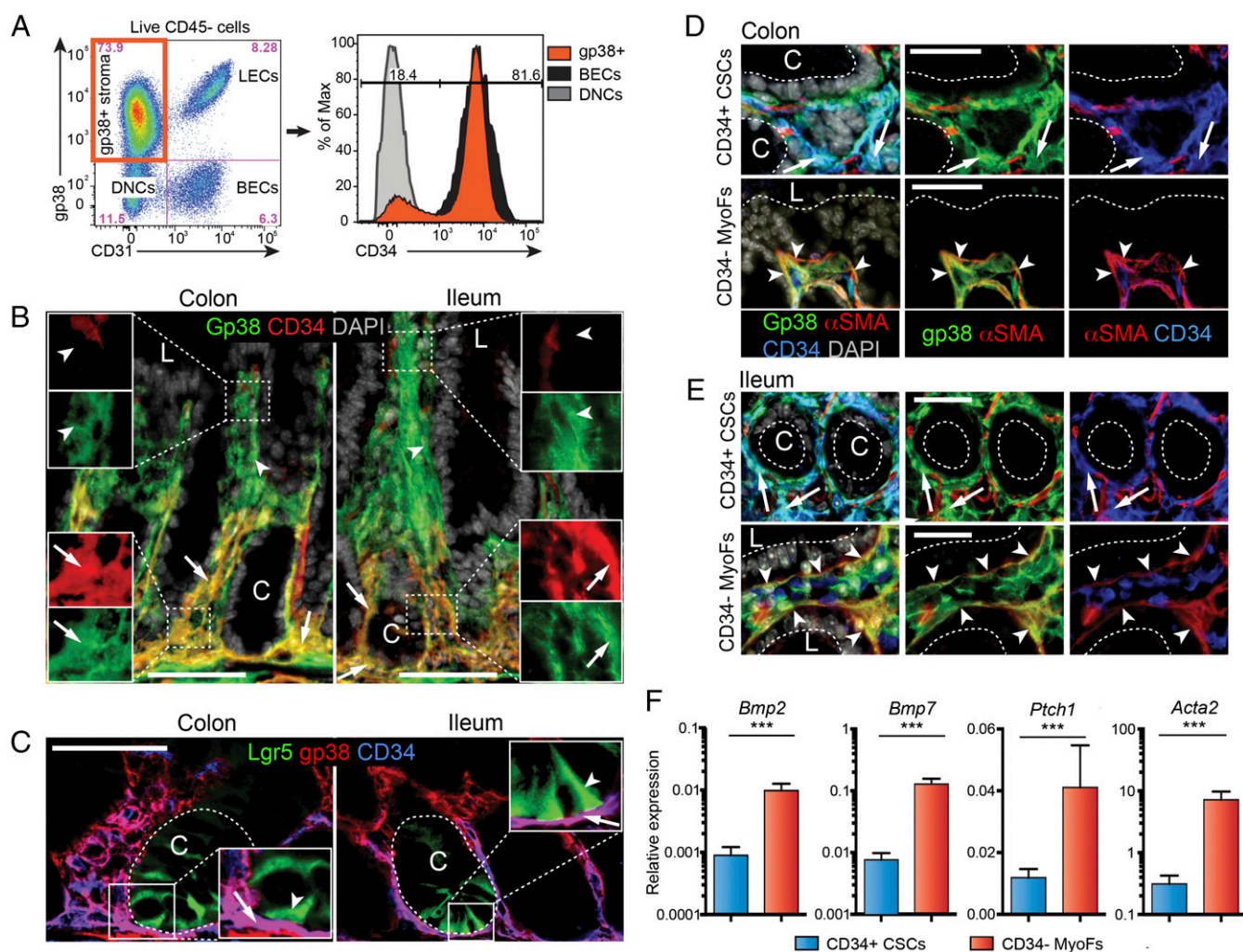


Fig. 1. Coexpression of gp38 and CD34 identifies pericryptal α SMA⁻ mesenchymal cells. (A) FACS plot and percentage of nonhematopoietic (CD45⁻) cells from the colonic lamina propria expressing gp38 and CD31 (Left) and analysis of CD34 expression (Right). BECs, blood endothelial cells; DNCs, double negative gp38⁺CD31⁻ cells; LECs, lymphatic endothelial cells. A plot representative of 10 independent experiments is shown. (B) Immunofluorescence analysis of gp38 (green) and CD34 (red) expression in mice colon (Left) and ileum (Right). Arrows indicate double positive gp38⁺CD34⁺ cells (appearing in orange/yellow) in crypts, and arrowheads indicate gp38⁺ CD34⁻ cells (appearing in green) in the villi and colon tops. (C) Immunofluorescence analysis of Lgr5 (green), gp38 (red), and CD34 (blue) expression in colon (Left) and ileum (Right) of Lgr5-egfp mice. Arrows indicate gp38⁺CD34⁺ cells in close contact with Lgr5⁺ cells (arrowheads). (D and E) Immunofluorescence analysis of gp38 (green), α SMA (red), and CD34 (blue) expression in colon (D) and ileum (E). Arrows indicate gp38⁺CD34⁺ α SMA⁻ cells (CD34⁺ CSCs; Upper); arrowheads indicate gp38⁺CD34⁻ α SMA⁺ cells (CD34⁻ MyoFs; Lower). (F) Expression of the indicated genes, as measured by qRT-PCR, in the indicated populations. $n = 8$ mice from three independent experiments. Values are mean \pm SD. In B–E, representative images of $n = 3$ –6 independent experiments are shown. DAPI stains nuclei. (Scale bars: B and C, 50 μ m; D and E, 25 μ m). *** $P < 0.001$.

transcripts coding for *Bmp2*, *Bmp7*, *Acta2* (coding for α SMA), and the Hedgehog receptor Patched (*Ptch1*) (13, 25), compared with CD34⁻ MyoFs (Fig. 1F). These results show that CD34⁺ CSCs are localized near crypts, adjacent to Lgr5⁺ IESCs, and express significantly lower levels of transcripts coding for genes involved in epithelial differentiation compared with CD34⁻ MyoFs.

CD34⁺ CSCs Promote IESCs Maintenance. The localization of CD34⁺ CSCs close to Lgr5⁺ IESCs (Fig. 1C) suggests a role in supporting IESC function. To test this hypothesis, we used a 3D Matrigel culture system that allows for the growth of intestinal crypts into organoids (27). In the absence of mesenchymal cells, crypts containing IESCs spontaneously formed self-organizing organoids when EGF and Rspo1 were added to the medium (Fig. 2A, Left). These structures contained budding crypts and epithelial cell shedding into the lumen. The addition to intestinal crypts of CD34⁺ CSCs isolated from mouse colon or ileum, but not of CD34⁻ myoFs, led to the formation of spherical structures, termed spheroids, with no visible crypts nor epithelial cell shedding (Fig. 2A and Fig. S2A). Fully differentiated intestinal organoids contained Ki-67⁺ proliferating cells restricted to the

crypts (Fig. 2B, Left), whereas spheroids contained a significantly higher proportion of Ki-67⁺ cells that were homogeneously distributed throughout the structure (Fig. 2B, Right; and C), indicating that CD34⁺ CSCs promote epithelial proliferation. Moreover, spheroids harbored fewer wheat germ agglutinin (WGA)-binding cells, such as Paneth cells and goblet cells, compared with organoids (Fig. 2D), suggesting that CD34⁺ CSCs impair epithelial differentiation.

To determine whether CD34⁺ CSCs affect the activity of Lgr5⁺ IESCs, normally restricted to crypts in fully differentiated organoids (27), we cocultured CD34⁺ CSCs with crypts isolated from Lgr5-EGFP mice (1). Spheroids induced by CD34⁺ CSCs contained a significantly higher proportion of Lgr5⁺ stem cells (up to 30%) compared with organoids grown without mesenchymal cells (2%) (Fig. 2E). Besides, IESCs growing in spheroids expressed higher levels of *Lgr5* (Fig. 2F), a Wnt target gene (9), suggesting that CD34⁺ CSCs increase the Wnt/ β -catenin signaling in IESCs.

CD34⁺ CSCs Maintain IESCs Through Secretion of Grem1 and Rspo1. The Wnt agonists *Wnt2b* and *Rspo1*, and the BMP antagonist *Grem1*, play a pivotal role in the maintenance of IESCs (7, 10, 11). We observed that CD34⁺ CSCs expressed significantly higher levels of *Grem1*, *Wnt2b*, and *Rspo1* compared with lamina propria CD34⁻ MyoFs, gp38⁺ CD34⁻ stromal cells (DNCs), endothelial cells (ECs), or leukocytes (Fig. 3A and Fig. S2B). Spheroid formation induced by CD34⁺ CSCs was markedly reduced in the presence of neutralizing anti-*Grem1* antibodies (Fig. 3B), indicating that *Grem1* production by CD34⁺ CSCs play a critical role in this process. Furthermore, crypts grown in the presence of CD34⁺ CSCs did not require supplementation with *Rspo1* (Fig. 3C), necessary for the growth of intestinal crypts, suggesting that CD34⁺ CSCs are an important source of *Rspo1*. Finally, transwell experiments confirmed that soluble factors were sufficient for the prostemness function of CD34⁺ CSCs (Fig. 3D and Fig. S2A), and that other stromal cells, such as skin fibroblasts, cannot compensate for the lack of CD34⁺ CSCs (Fig. 3D). Remarkably, maintenance of IESCs by CD34⁺ CSCs required their continuous presence, because spheroids rapidly differentiated into organoids when removed from CD34⁺ CSCs-containing medium (Fig. 3E). These results show that continuous supply of soluble niche factors by CD34⁺ CSCs is necessary and sufficient to promote IESC expansion. In agreement with these results, CD34⁺ CSCs express the transcription factor *Foxl1*, which was recently used as a marker to deplete intestinal mesenchymal cells with an essential role in maintenance of the IESC niche (28), and do not express *Myh11*, which identifies intestinal myofibroblasts with dispensable Wnt activity for the niche (18) (Fig. S3).

CD34⁺ CSCs Develop After Birth and Expand Around Crypts After Weaning. Crypts isolated from fetal mouse intestine form spontaneously spheroids, a potential that is rapidly lost after birth (29), suggesting that postnatal IESCs become dependent on external factors. Accordingly, crypts mature between embryonic day (E) 16.5 and the first weeks after birth (30). Whereas E16.5 embryos displayed clusters of gp38⁺ CD34⁻ stromal cells at sites of intestinal villus formation (Fig. 4A, Left and Fig. S4), gp38⁺ CD34⁺ stromal cells were absent from fetal or neonatal intestines. Gp38⁺ CD34⁺ stromal cells were detected in the first weeks after birth in the submucosa underlying colon crypts (Fig. 4A, Center) and were accounting for nearly one-half of the total gp38⁺ intestinal stromal cells 2 wk after birth (Fig. 4B). Submucosal gp38⁺ CD34⁺ cells at 2 wk expressed similar levels of *Grem1* than their adult counterparts, whereas expression of *Rspo1* and *Wnt2b* were still low (Fig. 4C), suggesting that these cells are immature CD34⁺ CSCs. During the third week after birth, the percentage of gp38⁺ CD34⁺ cells among total intestinal

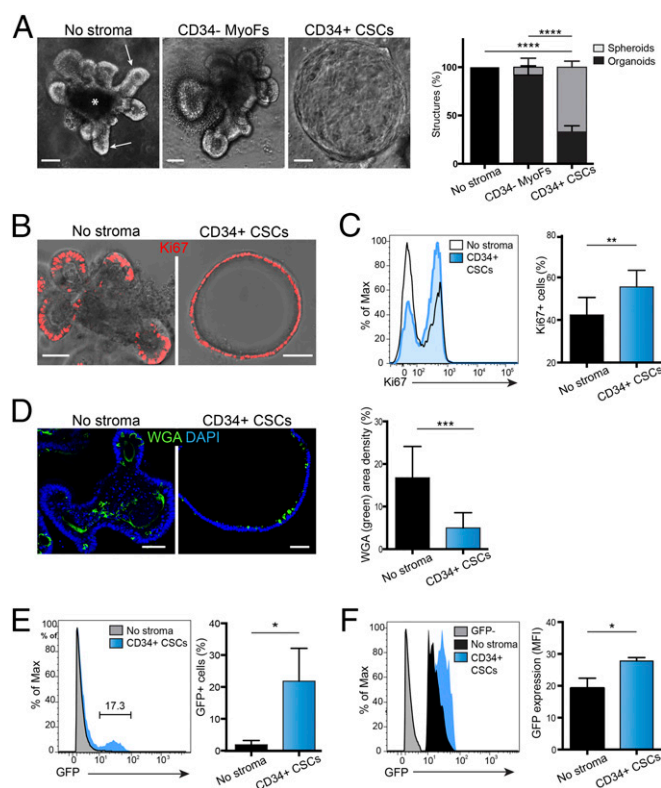


Fig. 2. CD34⁺ CSCs support IESCs proliferation. (A) Bright field microscopy analysis (Left) and percentage of organoids versus spheroids (Right) among intestinal structures grown in the indicated conditions for 5 d. Arrows indicate budding crypts, and an asterisk indicates organoid lumen; $n = 4$ from three independent experiments. (B) Confocal analysis of Ki-67 (red) expression in intestinal structures grown as described in A. (C) Intracellular FACS analysis of Ki-67 in organoids grown as indicated. $n = 6$ from two independent experiments. (D) Confocal analysis (Left) and quantification (Right) of WGA expression (green) in intestinal structures in indicated conditions. $n = 8$ from two independent experiments. (E) Percentage of GFP⁺ cells, as measured by FACS, in organoids harvested from *Lgr5-egfp* mice and grown as indicated; $n = 6$ from two independent experiments. (F) FACS analysis of GFP reporting Lgr5 expression in intestinal structures obtained from *Lgr5-egfp* mice and grown as indicated; $n = 6$ from two independent experiments. In A and C–F, values are mean \pm SD. (Scale bars: 100 μ m.) DAPI stains nuclei. **** $P < 0.0001$, *** $P < 0.001$, ** $P < 0.005$, * $P < 0.05$.

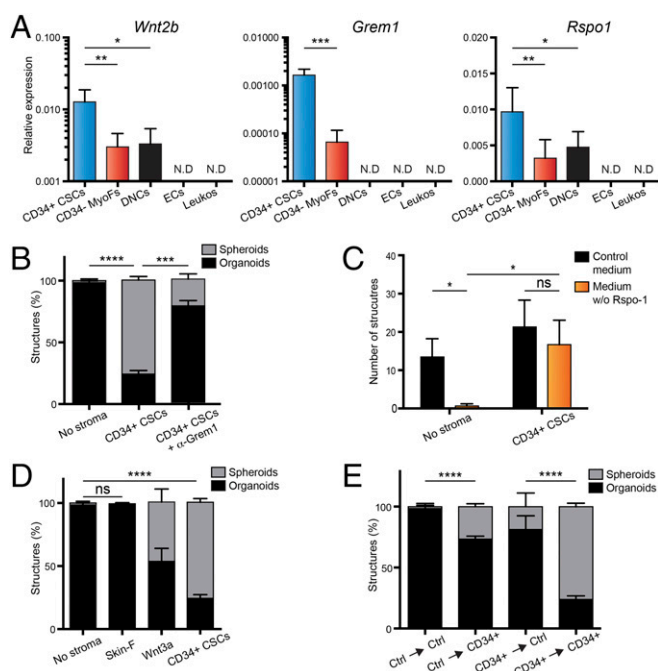


Fig. 3. CD34⁺ CSCs induce spheroids through secretion of Grem1 and Rspo1. (A) Expression of the indicated genes, as measured by qRT-PCR, in the indicated intestinal populations isolated by FACS from mouse colon. $n = 3$ –5 mice from two independent experiments. DNCs, double negative cells (gp38⁺CD31⁻); ECs, endothelial cells (CD31⁺); Leukos, hematopoietic cells (CD45⁺); ND, nondetected. (B) Percentage of spheroids vs. organoids obtained in 5-d cultures, supplemented with anti-gremlin1 blocking antibodies (α -Grem1); $n = 4$, from four independent experiments. (C) Total numbers of intestinal structures (organoids or spheroids) obtained after 2 d of culture without stromal cells, or with addition of CD34⁺ CSCs. $n = 3$, from two independent experiments. (D) Percentage of spheroids and organoids obtained in a transwell experiment after 5 d of culture in the indicated conditions. $n = 4$ from two independent experiments. (E) Percentage of spheroids and organoids obtained 48 h after transferring 5-d intestinal structures to the indicated conditions. CD34⁺, complete medium containing CD34⁺ CSCs; Ctrl, complete medium. $n = 3$ from two independent experiments. Values are mean \pm SD. **** $P < 0.0001$, *** $P < 0.001$, ** $P < 0.005$, * $P < 0.05$. ns, not significant.

gp38⁺ stromal cells increased markedly (Fig. 4B), and such an increase coincided with appearance of gp38⁺ CD34⁺ cells around the crypts (Fig. 4A, Right). Expansion and pericryptal localization of CD34⁺ CSCs was independent of intestinal colonization by microbiota and recognition of MAMPs, which in mice increase massively around weaning age (Fig. S5A), suggesting that development of CD34⁺ CSCs follows an ontogenic program. Consistent with our findings that CD34⁺ CSCs are a major intestinal source of Grem1 (Fig. 3A), *Grem1* expression was first detected in the submucosa and then near the crypts at 3 wk of life (Fig. S5B). These data show that gp38⁺ CD34⁺ stromal cells expressing high levels of *Grem1* develop in the intestinal submucosa during the first weeks after birth, and then are mostly localized around the crypts after 3 wk of age.

Intestinal Injury Induces Remodeling and Activation of CD34⁺ CSCs.

Intestinal injury induces an inflammatory response and repair process to control infection and regenerate the damaged epithelial layer. To determine the role of CD34⁺ CSCs during intestinal inflammation, we analyzed the intestine of adult mice subjected to DSS-mediated colitis. DSS induced damage and loss of colonic epithelial layer integrity (blue asterisk in Fig. 5A, Left), triggering regeneration of the epithelial layer in the following weeks (white asterisk in Fig. 5A, Right). Seven days after initiation

of DSS treatment, damaged zones were filled with an abundant scar tissue containing CD34⁺ CSCs near regenerating crypts (arrow in Fig. 5A, Left), whereas CD34⁻ MyoFs expanded in colon tops (arrowhead in Fig. 5A, Left). The proportion of CD34⁺ CSCs among total gp38⁺ stromal cells decreased during inflammation, reaching preweaning levels (Fig. 5B). CD34⁺ CSCs isolated from DSS-inflamed colon overexpressed niche factors *Grem1* and *Rspo1*, compared with CD34⁺ CSCs at steady state, suggesting that their prostemness function is maintained during intestinal inflammation (Fig. 5D). Inflamed CD34⁺ CSCs also strongly up-regulated *Vcam1* (Fig. 5C), an adhesion molecule expressed by mesenchymal stromal cells in lymphoid organs, which is essential for the recruitment of immune cells. In addition, CD34⁺ CSCs isolated from acutely inflamed colon significantly overexpressed, compared with CD34⁺ CSCs at steady state, transcripts coding for *Ccl2* (*Mcp-1*) and *Csf1* (*M-csf*); essential for the recruitment of monocytes and macrophages to inflamed tissues and for macrophage maintenance, respectively; the neutrophil chemoattractants *Cxcl1* and *Cxcl2*; the proinflammatory cytokine *Il6*; as well as *Ccl19*, *Cxcl13*, *Icam1*, *Trance* (*Rankl*), and *Tnfr1*, all involved in the organization of adaptive immune responses; and the lymphangiogenic growth factors *Vegfc*, *Vegfd*, and *Fgf2* (Fig. 5D). Finally, CD34⁺ CSCs up-regulated a number of growth factors for epithelial cells such as *Areg* (*Amphiregulin*), *Fgf7*, *Fgf10*, as well as *Ptgs2*, which modulates epithelial proliferation through effects on prostaglandin synthesis (31), and *Col1a1* (coding for type I collagen), suggesting a direct role in epithelial proliferation and tissue repair. Overexpression by CD34⁺ CSCs of most proinflammatory molecules was transient, peaking during the acute phase of inflammation, with a few notable exceptions including the T cells and DCs chemotactic factor *Ccl19*, and the lymphocyte survival factor *Il7*, which are key factors of adaptive immunity (Fig. 5D). Consistent with a role in adaptive immunity, CD34⁺ CSCs isolated from the colon supported T-cell survival in vitro (Fig. S6). Finally, a number of transcripts were overexpressed in CD34⁻ MyoFs compared with CD34⁺ CSCs, including, in addition to BMPs, transcripts coding for genes involved in vasculature growth and remodeling such as *Angpt1*, *Angpt2*, and *Vegfa*, as well as *Wnt5a*, a noncanonical Wnt ligand that plays an essential role in intestinal regeneration (32), suggesting that intestinal homeostasis and repair require the coordinated action of functionally distinct subsets of mesenchymal cells (a scheme is shown in Fig. S7).

Discussion

Here, we identify CD34⁺ CSCs as the major intestinal source for the IESC niche factors *Wnt2b*, *Grem1*, and *Rspo1*. CD34⁺ CSCs are closely adjacent to Lgr5⁺ IESCs, both in colon and ileum, and are sufficient to promote expansion of Lgr5⁺ IESCs in organoids, an effect mainly dependent on Grem1. CD34⁺ CSCs are topographically and functionally distinct from α SMA⁺ subepithelial myofibroblasts, and develop after birth in the intestinal submucosa, independently of the microbiota. We further show that, after intestinal damage and inflammation, CD34⁺ CSCs remain in close proximity to regenerating crypts and up-regulate Grem1 and Rspo1, as well as a number of chemokines, cytokines, and growth factors with key roles in intestinal immunity and tissue repair. CD34⁺ CSCs are therefore an essential component of the IESC niche at homeostasis and contribute to intestinal inflammation and repair after damage.

Wnt signaling is required to maintain IESCs (4). Paneth cells are the main source for the Wnt ligand Wnt3 and play an important role in the IESC niche (5). However, mice lacking Wnt activity in epithelial cells or myofibroblastic cells have normal intestinal homeostasis, and ablation of Paneth cells does not affect the function of IESCs (16–18), suggesting redundant or compensatory mechanisms involving nonepithelial and non-myofibroblastic sources. In agreement with this hypothesis, CD34⁺

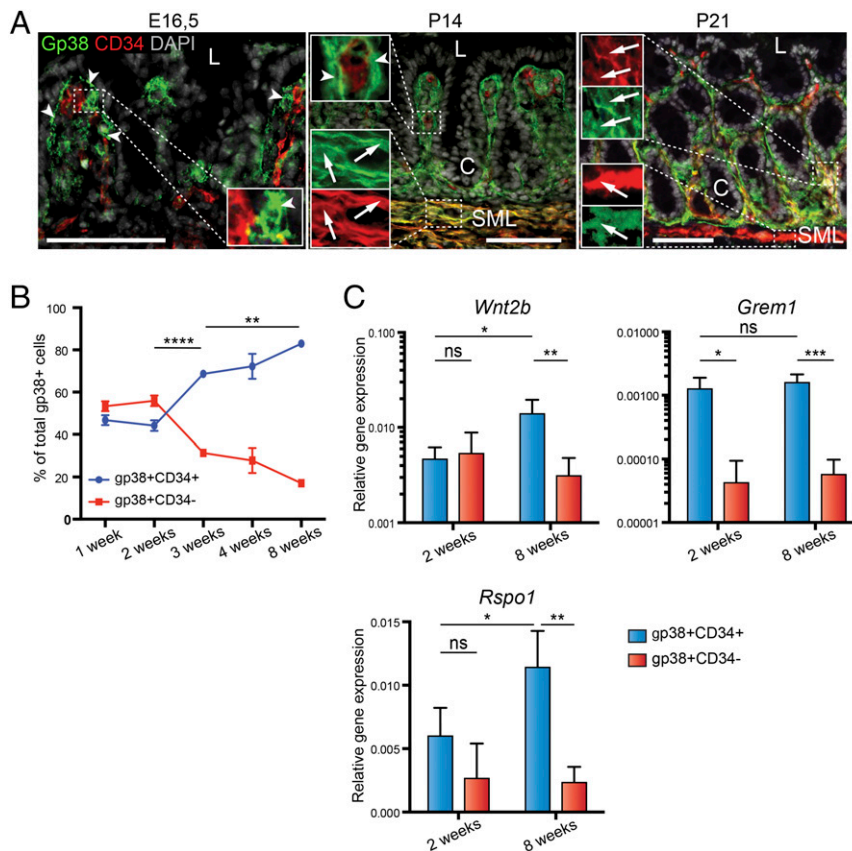


Fig. 4. CD34⁺ CSCs expand in the submucosal layer and the pericryptal niche after weaning. (A) Immunofluorescence analysis of gp38 (green) and CD34 (red) expression by lamina propria stromal cells at E16.5 (embryonic age after conception), and 14 d (P14) or 21 d (P21) after birth. *Insets* show gp38⁺ CD34⁻ stromal cells (arrowheads) and gp38⁺ CD34⁺ stromal cells (arrows); images are representative of $n = 4$ mice from three independent experiments. C, crypt; L, lumen; SML, submucosal layer. Costaining with CD31 confirmed that fetal and postnatal gp38⁻ CD34⁺ cells are blood vessels (Fig. S4). (Scale bar: 50 μ m.) (B) FACS analysis of CD34⁺ and CD34⁻ cells among CD45⁻ CD31⁻ gp38⁺ intestinal stromal cells at the indicated time after birth; $n = 4$ mice from two independent experiments. (C) Expression of the indicated genes, as measured by qRT-PCR, in CD34⁺ and CD34⁻ stromal cells isolated by FACS from colons of 2- and 8-wk-old mice. $n = 3$ –5 mice from two independent experiments. DAPI stains nuclei. In B and C, values are mean \pm SD. **** $P < 0.0001$, *** $P < 0.001$, ** $P < 0.005$, * $P < 0.05$. ns, not significant.

CSCs express high levels of *Wnt2b*, which is sufficient to compensate for the loss of Paneth cells-derived *Wnt3* (7); *Rspo1*, which supports canonical Wnt signaling in crypts by binding to *Lgr4/5* receptors (8–10) and synergizes with secreted Wnt proteins (8, 33); and *Grem1*, which favors Wnt signaling by antagonizing BMPs (12). These data are consistent with the previously reported expression of *Wnt2b* and *Grem1* by intestinal mesenchyme (7, 11), and of an ill-defined intestinal mesenchyme supporting IESC growth in vitro (34). We further show that inhibition of *Grem1* significantly reduces the generation of CD34⁺ CSC-induced spheroids, indicating that secretion of *Grem1* by CD34⁺ CSCs plays a predominant role in maintenance of IESCs. Consistent with this hypothesis, forced expression of *Grem1* in epithelial cells is sufficient to disrupt intestinal morphogenic gradients, promoting the persistence or reacquisition of stem cell properties by differentiated epithelial cells (35). The massive epithelial proliferation observed in CD34⁺ CSC-induced spheroids is therefore consistent with a global activation of Wnt signaling, normally restricted to the crypts (36). In the colon, which lacks Paneth cells, CD34⁺ CSCs production of *Wnt2b*, *Rspo1*, and *Grem1* may therefore represent the major source of niche signals supporting IESCs. Accordingly, depletion of intestinal mesenchymal cells expressing the transcription factor *Foxl1* (28), also expressed by CD34⁺ CSCs, is sufficient to severely affect crypt proliferation.

We further show that CD34⁺ CSCs are topographically and functionally distinct from α SMA⁺ subepithelial myofibroblasts,

identified as gp38⁺ CD34⁻ α SMA^{high} (CD34⁻ MyoFs), which are located beneath epithelial cells in the ileum villi and colon tops. CD34⁺ CSCs develop after birth, in contrast to CD34⁻ MyoFs that are already present in fetal and neonatal intestine. Postnatal gp38⁺ CD34⁺ cells are first detected in the intestinal submucosa, then around the crypts starting at 3 wk after birth. Because they express high levels of *Grem1*, postnatal CD34⁺ cells may play a role in intestinal crypt maturation during the first few weeks after birth, characterized by the rapid increase in crypt numbers (37) and Paneth cells maturation (38), two processes that require Wnt signaling. The increase in number and pericryptal localization of CD34⁺ CSCs is independent of the microbial colonization of the gut, which massively increases at 3 wk of age in mice, suggesting that postnatal IESC mesenchymal niche is developmentally regulated. By occupying the pericryptal niche in the lamina propria, CD34⁺ CSCs might prevent BMP-producing CD34⁻ MyoFs from expanding into the crypts and disrupting homeostasis of stem cells. Thus, development and specific positioning of two distinct mesenchymal populations in the intestinal villi and crypts might be critical to maintain the pool of IESCs, and to promote directional differentiation of villous epithelial cells. Nevertheless, whether CD34⁻ MyoFs and CD34⁺ CSCs have a common progenitor, or whether one population is generated from the other, remains to be investigated.

Intestinal damage induces a coordinated inflammatory response and tissue repair to regenerate the intestinal epithelial

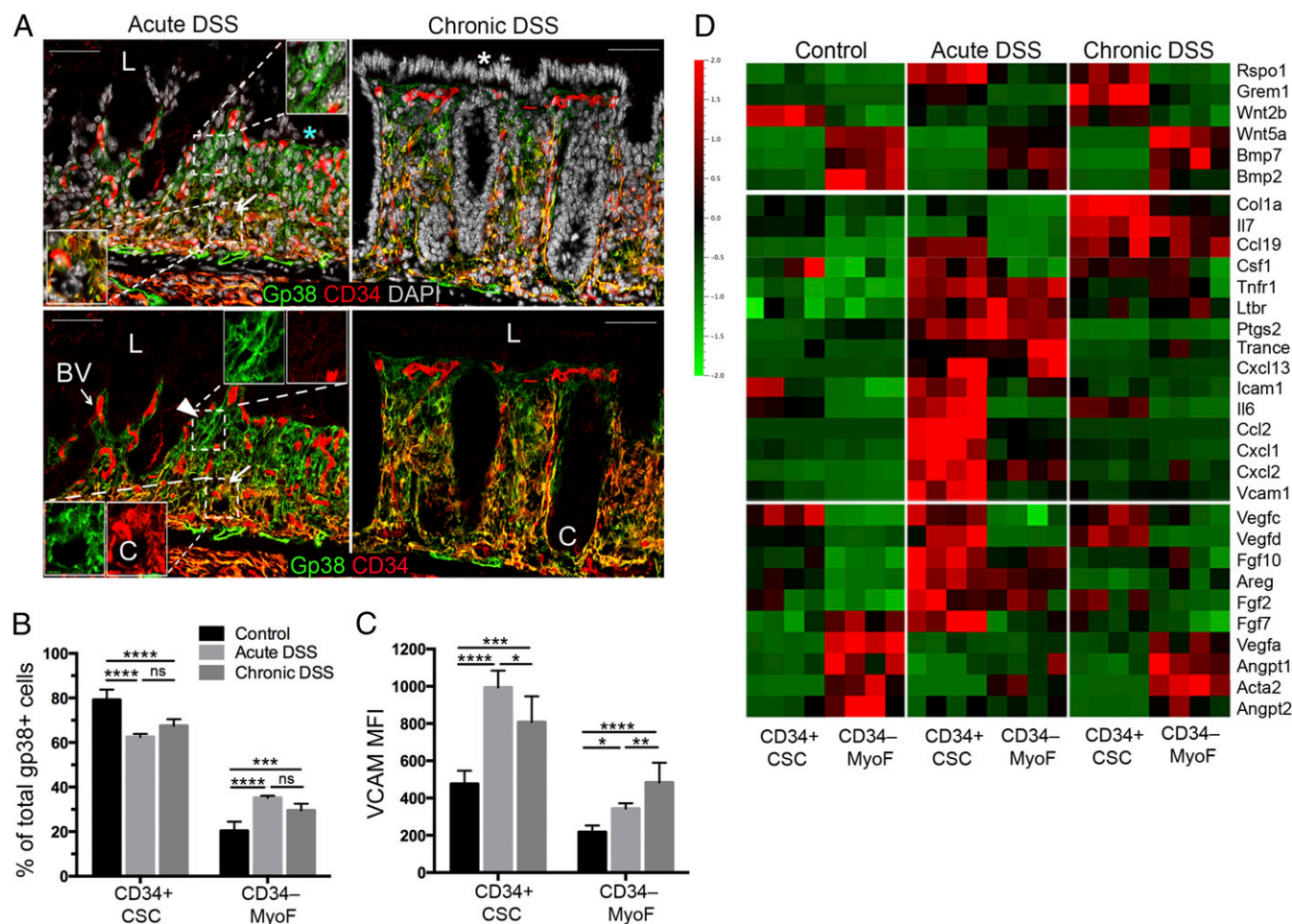


Fig. 5. Intestinal inflammation induces remodeling and activation of CD34⁺ CSCs. (A) Immunofluorescence analysis of gp38 (green) and CD34 (red) expression by intestinal stromal cells after acute or chronic DSS-induced colitis. *Insets* show bigger magnification of CD34⁺ CSCs (arrow) or CD34⁻ MyoFs (arrowhead) in acute DSS. BV, blood vessels; C, crypts; L, lumen. (Scale bar: 50 μ m). (B) Percentage of CD34⁺ and CD34⁻ cells among total gp38⁺ stromal cells (gated CD45⁻ CD31⁻) obtained by FACS at steady state, or after acute DSS and chronic DSS. (C) Mean fluorescence intensity (MFI) of Vcam1 expression by CD34⁺ CSCs and CD34⁻ MyoFs in the indicated conditions. (D) Clustered gene expression analysis, as measured by qRT-PCR, for CD34⁺ CSCs and CD34⁻ MyoFs in the indicated conditions. $n = 4-6$ for each condition from two to three independent experiments. DAPI stains nuclei. In B and C, values are mean \pm SD. **** $P < 0.0001$, *** $P < 0.001$, ** $P < 0.005$, * $P < 0.05$.

barrier and restore homeostasis. In lymphoid organs, specialized subsets of mesenchymal cells termed lymphoid stromal cells (mostly expressing gp38) are essential for leukocyte recruitment, cross-talk, and survival (19). Our results indicate that, during intestinal inflammation, CD34⁺ CSCs acquire characteristics of lymphoid stromal cells, such as expression of *Vcam1*, *Icam1*, and *Ltbr*, and the lymphocyte survival factor *Il-7*. The formation of clusters of LT β R⁺ Vcam1⁺ Icam1⁺ lymphoid stromal cells initiates lymphoid tissue genesis, because these adhesion molecules are essential to establish cell-cell contact between stromal cells and lymphotoxin-expressing lymphocytes (39, 40). Consistent with their production of *Il-7*, we found that CD34⁺ CSCs are sufficient to support T cells survival in vitro. In addition, CD34⁺ CSCs up-regulate expression of several chemokines involved in leukocyte trafficking and immune regulation, including *Ccl2*, which has a pivotal role in recruiting monocytes and macrophages to inflamed tissues, and *Csf1*, essential for macrophage maintenance. Because macrophages are necessary for crypt regeneration after injury (31), it is possible that CD34⁺ CSCs contribute to the maintenance and restoration of the IESC niche by several mechanisms, including secretion of niche factors at homeostasis and attraction of additional components of the IESC niche, such as macrophages, after injury. Expression by CD34⁺ CSCs of *Ptgs2* after injury, necessary for regenerative

responses after DSS-induced colitis (41), further supports this hypothesis.

Finally, given their central role in promoting proliferation of IESCs and inflammation, CD34⁺ CSCs may play a role in the pathogenesis of intestinal diseases such as inflammatory bowel disease and colon cancer. *Grem1* is overexpressed in carcinoma-associated fibroblasts of several human carcinomas, including colon carcinomas, and promotes tumor cell proliferation (42). Cocultures of intestinal organoids with CD34⁺ CSCs may therefore provide a relevant model to decipher the stromal cross-talk that is dysregulated in cancer or inflammatory diseases and to develop novel therapies targeting stromal cells. Conversely, manipulation of the endogenous mesenchymal niche might be beneficial to improve stem cells engraftment and survival, opening new avenues for regenerative medicine.

Materials and Methods

Mice. C57/B16J wild-type (WT) mice were purchased from Charles River. *Lgr5-egfp* mice (B6.129P2-*Lgr5*^{tm1(Cre/ESR1)C1eJ}) were purchased from Jackson Laboratories. *Myd88*^{-/-} *TRIF*^{-/-} mice were obtained from C. Werts, Institut Pasteur. All mice were kept in specific pathogen-free (SPF) conditions. Germ-free (GF) mice of the C57/B16J background (CDTA) were bred and maintained at the Institut Pasteur. To induce intestinal colitis, we treated 8- to 12-wk-old mice with 2.5% (wt/vol) dextran sodium sulfate (DSS) in the

drinking water for 7 d (acute model) or with one cycle of 2% (wt/vol) DSS during 7 d, followed by 7 d of water, one cycle of 2% (wt/vol) DSS during 7 d, and 7 d of water (chronic model). Mouse experiments were approved by the committee on animal experimentation of the Institut Pasteur and by the French Ministry of Agriculture.

Antibodies. The following monoclonal antibodies were purchased from eBiosciences: V500-conjugated CD45.2 (104), eFluor 605-conjugated Ki-67 (SolA15), eFluor 605-conjugated CD31 (390), and eFluor 660-conjugated CD34 (RAM34). Cy3-conjugated α -SMA-specific antibody (1A4) was purchased from Sigma. Purified rabbit GFP-specific antibody (A11122), Alexa 555-conjugated WGA, and Alexa 647-conjugated anti-rat IgG (H+L) were purchased from Invitrogen. Cy3-conjugated and Alexa 647-conjugated anti-syrian hamster were purchased from Jackson ImmunoResearch. Syrian hamster antibody to gp38 was a gift from A. Farr, University of Washington, Seattle.

Histology. Tissue processing and staining were performed as described (43). Briefly, the entire colon and ileum were washed in PBS, fixed overnight at 4 °C in 4% paraformaldehyde (Sigma-Aldrich), embedded in OCT compound (VWR Chemicals), and stored at -80 °C. Frozen blocks were cut at 8 μ m thickness, and sections were collected onto Superfrost Plus slides (VWR International). Sections were processed for antibody staining: After blocking with 10% (vol/vol) bovine serum in PBS, slides were incubated with primary antibodies overnight at 4 °C, washed three times for 5 min, incubated with secondary antibodies for 1 h at room temperature, washed once, incubated with DAPI (Sigma) for 5 min, washed three times for 5 min, and mounted with FluoromountG (Southern Biotechnology Associates). We examined slides with an AxioImager M1 or A2 (Apotome) fluorescence microscope (Zeiss) equipped with a CCD camera and processed images with AxioVision or Zen software (Zeiss).

Isolation of Intestinal Stromal Cells. To isolate intestinal stromal cells, we processed mouse ileum or colon as described (20). Briefly, after removal of Peyer's patches (from the ileum), epithelial cells were removed by incubating gut fragments in calcium and magnesium-free DMEM (Gibco) containing 10 mM EDTA for 20 min at 37 °C with gentle agitation. Gut pieces were washed and incubated in DMEM (Gibco) containing Liberase TL (1 unit/mL; Roche) and DNase I (1 unit/mL; Invitrogen) at 37 °C. After 20 min, the digested fraction was collected and put on ice. This cycle was repeated two additional times for a total digestion time of 60 min. The remaining intestinal fragments were collected, filtered through a 100- μ m mesh, and mixed with the collected supernatants.

Flow Cytometry. For FACS analysis, we first incubated cells with monoclonal antibody 2.4G2 to block Fc γ receptors, and then with indicated antibodies for 40 min in a total volume of 100 μ L of PBS containing 2 mM EDTA and 2% (vol/vol) bovine serum, followed by appropriate secondary antibodies for 30 min when necessary. Cells were incubated for 1 min with DAPI (Sigma) before analysis to exclude dead cells. For intracellular staining of α -SMA and Ki-67, we fixed and permeabilized cells at room temperature (RT), then stained with antibodies in PBS-IF for 60 min at RT. Cell were analyzed with Fortessa (BD Biosciences) and Flowjo software (Tristar). Fluorescence intensity is expressed in arbitrary units on a logarithmic scale or on a linear scale for forward and side scatter. Cells were sorted with FACS Aria 3 (BD Biosciences) by using a single-cell sorting mask.

RNA Isolation and Quantitative RT-PCR. We performed RNA isolation and quantitative RT-PCR (qRT-PCR) as described (43). Briefly, we extracted total

RNA from FACS-sorted cells by using RNeasy Micro Kit (Qiagen) and assessed the quality of total RNA by using the 2100 Bioanalyzer system (Agilent Technologies). We used 250–500 pg of high-quality total RNA for one linear mRNA amplification cycle by using the MessageBooster kit for qRT-PCR (Epicentre Biotechnologies). Amplified mRNA (50–100 ng) was transcribed into cDNA by using SuperScript III reverse transcriptase (Invitrogen). All procedures were performed according to the manufacturers' protocols. We performed qRT-PCR by using RT²-qPCR primer sets (SABiosciences) and RT² SYBR-Green master mix (SABiosciences), on a PTC-200 thermocycler equipped with a Chromo4 detector (Bio-Rad Laboratories), and analyzed data by using Opticon Monitor software (Bio-Rad Laboratories). We normalized C_t values to the mean C_t values obtained for the housekeeping genes *Hsp90ab1*, *Hprt*, and *Gapdh*. Heat maps were generated by using Qlucore software.

Stromal Cells and Organoid Coculture. We isolated intestinal crypts as described (27). Briefly, we isolated small intestines, flushed with cold PBS, opened longitudinally, and removed villi. We cut tissues into 1-cm pieces and incubated in PBS containing 10 mM EDTA on ice for 30 min. We filtered crypts-containing supernatants and counted. We mixed a total of 250 crypts with 5 \times 10⁴ stromal cells isolated by FACS from mouse intestine and embedded in matrigel (Corning). After polymerization, we added crypt medium (CM) composed of DMEM/F12 supplemented with 10% (vol/vol) bovine serum, 100 U/mL penicillin/streptomycin, 10 mM HEPES, 1 \times N2, 1 \times B27 (Gibco), 50 ng/mL EGF (Peprotech), and 100 ng/mL Noggin (Peprotech). When indicated, we added 500 ng/mL R-spondin1 (R&D) to the medium. After 2 or 5 d, we counted intestinal organoids by using an inverted bright field microscope and imaged by using an Olympus IX81 with the CellSense software.

Transwell Assays. We isolated intestinal stromal cells by FACS and plated in complete medium at a concentration of 1 \times 10⁵ cells per well. When cells reached 50% confluency, we added a transwell filter containing intestinal crypts in Matrigel, as described above. After 5 d, we counted organoids by using an inverted bright field microscope and imaged by using an Olympus IX81 with the CellSense software.

Confocal Microscopy. For confocal microscopy analysis, we processed intestinal organoids as described (44). Organoids were sectioned with a HM650V vibratome (Thermo Fisher Scientific) and mounted with Prolong Gold Antifade reagent (Life Technologies). We acquired images by using a confocal microscope (sp5, Leica; or Cell Voyager CV1000, Yokogawa) and analyzed with ImageJ. We applied a Z projection by using average intensity to the z stacks and binarized images by using the OTSU threshold.

T-Cell Survival. We plated intestinal stromal cells isolated by FACS 96-well plates in DMEM containing penicillin (50 IU/mL), streptomycin (50 μ g/mL), and 10% (vol/vol) FBS (Sigma). After 5 d, we added 2 \times 10⁵ T cells purified by magnetic-activated cell sorting to stromal cells. Recombinant IL-7 was used at 1 ng/ μ L in the absence of stromal cells. After 60 h of coculture, we collected lymphocytes to analyze living cells by FACS analysis.

ACKNOWLEDGMENTS. This project has received funding from the Institut Pasteur, la Fondation pour la Recherche Médicale (to G.E.), and the European Research Council (ERC) Consolidator Grant 648428-PERIF (to L.P.). I.S. was funded by the Ministère de l'Enseignement Supérieur et de la Recherche and the Fondation pour la Recherche Médicale en France Grant FDT20130928338. J.-M.J. was funded by the Ministère de l'Enseignement Supérieur et de la Recherche. P.J.S. received funding from European Research Council Advanced Grant 339579-DECRYPT.

- Barker N, et al. (2007) Identification of stem cells in small intestine and colon by marker gene Lgr5. *Nature* 449(7165):1003–1007.
- van der Flier LG, Clevers H (2009) Stem cells, self-renewal, and differentiation in the intestinal epithelium. *Annu Rev Physiol* 71:241–260.
- Pinto D, Gregorieff A, Begthel H, Clevers H (2003) Canonical Wnt signals are essential for homeostasis of the intestinal epithelium. *Genes Dev* 17(14):1709–1713.
- Kuhnert F, et al. (2004) Essential requirement for Wnt signaling in proliferation of adult small intestine and colon revealed by adenoviral expression of Dickkopf-1. *Proc Natl Acad Sci USA* 101(1):266–271.
- Sato T, et al. (2011) Paneth cells constitute the niche for Lgr5 stem cells in intestinal crypts. *Nature* 469(7330):415–418.
- van Es JH, et al. (2005) Notch/gamma-secretase inhibition turns proliferative cells in intestinal crypts and adenomas into goblet cells. *Nature* 435(7044):959–963.
- Farin HF, Van Es JH, Clevers H (2012) Redundant sources of Wnt regulate intestinal stem cells and promote formation of Paneth cells. *Gastroenterology* 143(6):1518–1529.e7.
- Kim KA, et al. (2005) Mitogenic influence of human R-spondin1 on the intestinal epithelium. *Science* 309(5738):1256–1259.
- de Lau W, et al. (2011) Lgr5 homologues associate with Wnt receptors and mediate R-spondin signalling. *Nature* 476(7360):293–297.
- Ootani A, et al. (2009) Sustained in vitro intestinal epithelial culture within a Wnt-dependent stem cell niche. *Dev Med* 15(6):701–706.
- Kosinski C, et al. (2007) Gene expression patterns of human colon tops and basal crypts and BMP antagonists as intestinal stem cell niche factors. *Proc Natl Acad Sci USA* 104(39):15418–15423.
- Hsu DR, Economides AN, Wang X, Eimon PM, Harland RM (1998) The Xenopus dorsalizing factor Gremlin identifies a novel family of secreted proteins that antagonize BMP activities. *Mol Cell* 1(5):673–683.
- He XC, et al. (2004) BMP signaling inhibits intestinal stem cell self-renewal through suppression of Wnt-beta-catenin signaling. *Nat Genet* 36(10):1117–1121.
- Haramis AP, et al. (2004) De novo crypt formation and juvenile polyposis on BMP inhibition in mouse intestine. *Science* 303(5664):1684–1686.

15. Powell DW, Pinchuk IV, Saada JI, Chen X, Mifflin RC (2011) Mesenchymal cells of the intestinal lamina propria. *Annu Rev Physiol* 73:213–237.
16. Kabiri Z, et al. (2014) Stroma provides an intestinal stem cell niche in the absence of epithelial Wnts. *Development* 141(11):2206–2215.
17. Durand A, et al. (2012) Functional intestinal stem cells after Paneth cell ablation induced by the loss of transcription factor Math1 (Atoh1). *Proc Natl Acad Sci USA* 109(23):8965–8970.
18. San Roman AK, Jayewickreme CD, Murtaugh LC, Shivdasani RA (2014) Wnt secretion from epithelial cells and subepithelial myofibroblasts is not required in the mouse intestinal stem cell niche in vivo. *Stem Cell Rep* 2(2):127–134.
19. Peduto L, et al. (2009) Inflammation recapitulates the ontogeny of lymphoid stromal cells. *J Immunol* 182(9):5789–5799.
20. Stzpourginski I, Eberl G, Peduto L (2015) An optimized protocol for isolating lymphoid stromal cells from the intestinal lamina propria. *J Immunol Methods* 421:14–19.
21. Breiteneder-Geleff S, et al. (1999) Angiosarcomas express mixed endothelial phenotypes of blood and lymphatic capillaries: Podoplanin as a specific marker for lymphatic endothelium. *Am J Pathol* 154(2):385–394.
22. Fina L, et al. (1990) Expression of the CD34 gene in vascular endothelial cells. *Blood* 75(12):2417–2426.
23. Crisan M, et al. (2008) A perivascular origin for mesenchymal stem cells in multiple human organs. *Cell Stem Cell* 3(3):301–313.
24. Vanderwinden JM, Rumessen JJ, De Laet MH, Vanderhaeghen JJ, Schiffmann SN (2000) CD34 immunoreactivity and interstitial cells of Cajal in the human and mouse gastrointestinal tract. *Cell Tissue Res* 302(2):145–153.
25. van Dop WA, et al. (2009) Depletion of the colonic epithelial precursor cell compartment upon conditional activation of the hedgehog pathway. *Gastroenterology* 136(7):2195–2203.e1, 7.
26. Madison BB, et al. (2005) Epithelial hedgehog signals pattern the intestinal crypt-villus axis. *Development* 132(2):279–289.
27. Sato T, et al. (2009) Single Lgr5 stem cells build crypt-villus structures in vitro without a mesenchymal niche. *Nature* 459(7244):262–265.
28. Aoki R, et al. (2016) Foxl1-expressing mesenchymal cells constitute the intestinal stem cell niche. *Cell Mol Gastroenterol Hepatol* 2(2):175–188.
29. Mustata RC, et al. (2013) Identification of Lgr5-independent spheroid-generating progenitors of the mouse fetal intestinal epithelium. *Cell Reports* 5(2):421–432.
30. Gregorieff A, Clevers H (2005) Wnt signaling in the intestinal epithelium: From endoderm to cancer. *Genes Dev* 19(8):877–890.
31. Pull SL, Doherty JM, Mills JC, Gordon JI, Stappenbeck TS (2005) Activated macrophages are an adaptive element of the colonic epithelial progenitor niche necessary for regenerative responses to injury. *Proc Natl Acad Sci USA* 102(1):99–104.
32. Miyoshi H, Ajima R, Luo CT, Yamaguchi TP, Stappenbeck TS (2012) Wnt5a potentiates TGF- β signaling to promote colonic crypt regeneration after tissue injury. *Science* 338(6103):108–113.
33. Kazanskaya O, et al. (2004) R-Spondin2 is a secreted activator of Wnt/beta-catenin signaling and is required for *Xenopus* myogenesis. *Dev Cell* 7(4):525–534.
34. Lei NY, et al. (2014) Intestinal subepithelial myofibroblasts support the growth of intestinal epithelial stem cells. *PLoS One* 9(1):e84651.
35. Davis H, et al. (2015) Aberrant epithelial GREM1 expression initiates colonic tumorigenesis from cells outside the stem cell niche. *Nat Med* 21(1):62–70.
36. van de Wetering M, et al. (2002) The beta-catenin/TCF-4 complex imposes a crypt progenitor phenotype on colorectal cancer cells. *Cell* 111(2):241–250.
37. Dehmer JJ, et al. (2011) Expansion of intestinal epithelial stem cells during murine development. *PLoS One* 6(11):e27070.
38. van Es JH, et al. (2005) Wnt signalling induces maturation of Paneth cells in intestinal crypts. *Nat Cell Biol* 7(4):381–386.
39. Bénézech C, et al. (2010) Ontogeny of stromal organizer cells during lymph node development. *J Immunol* 184(8):4521–4530.
40. Drayton DL, Liao S, Mounzer RH, Ruddle NH (2006) Lymphoid organ development: From ontogeny to neogenesis. *Nat Immunol* 7(4):344–353.
41. Brown SL, et al. (2007) Myd88-dependent positioning of Ptgs2-expressing stromal cells maintains colonic epithelial proliferation during injury. *J Clin Invest* 117(1):258–269.
42. Karagiannis GS, et al. (2015) Bone morphogenetic protein antagonist gremlin-1 regulates colon cancer progression. *Biol Chem* 396(2):163–183.
43. Dulauroy S, Di Carlo SE, Langa F, Eberl G, Peduto L (2012) Lineage tracing and genetic ablation of ADAM12(+) perivascular cells identify a major source of profibrotic cells during acute tissue injury. *Nat Med* 18(8):1262–1270.
44. Snippert HJ, et al. (2010) Intestinal crypt homeostasis results from neutral competition between symmetrically dividing Lgr5 stem cells. *Cell* 143(1):134–144.